NETWORK REPRESENTATION OF THE GAME OF LIFE

Yoshihiko Kayama and Yasumasa Imamura

Department of Media and Information, BAIKA Women's University,
2-19-5, Shukuno-sho, Ibaraki 567-8578, Osaka, Japan

Abstract

The Game of Life (Life) is one of the most famous cellular automata. The main purpose of this article is to present a network representation of Life as an application of the approach proposed in our previous papers. This network representation has made it possible to investigate Life using a network theory. Some well-known Life patterns are illustrated by using the corresponding clustered networks. The visualization of Life's *rest* state reveals the underlying tension as a complex network. The typical network parameters show the characteristics of Life as a Wolfram's class IV rule. In particular, the *in*-degree distribution of the derived network from a Life's rest state shows a scale-free nature, which could be related to the evidence of *self-organized criticality*.

1 Introduction

Conway's Game of Life [1], or simply Life, is one of the most famous cellular automata (CA), which are characterized by a number of cells on a lattice grid and a synchronous update of all cell states according to a local rule. Because Life's rule was carefully determined to balance the cells' tendencies to die and to be born, many complex patterns and activities can emerge [2]–[4].

The original concept of CA was introduced by von Neumann and Ulam for modeling biological self-reproduction [5]. Since their introduction, CA have been used in many disciplines including physics, computer science, biology, and social sciences [5]–[9]. Subsequently, S. Wolfram systematically investigated the dynamical behavior of one-dimensional cellular automata (1D CA) and proposed that the rules can be grouped into four classes of complexity: homogeneous (class I), periodic (class II), chaotic (class III), and complex (class IV) [10]. Life is not only a member of class IV, but it is also one of the simplest examples of what we call s*elf-organizing systems* or *self-organized criticality* (SOC) [11]. The concept of SOC was proposed by Bak, Tang and Wiesenfeld [12]. They discovered that the critical behavior can be emerged *sponta-*

neously from simple local interactions without any fine tunings of variable parameters.

In our previous papers [13, 14], we proposed a *network representation* that made it possible to describe the dot patterns of binary CA by network graphs. Each network has characteristic link patterns and symmetries derived from the dynamical behavior of the corresponding CA rule. For example, additive rules such as rule 90 of elementary cellular automata (ECA) and rule $T42$ of 5-neighbor totalistic cellular automata (5TCA) provide geometric links that are independent of initial configurations. Our network representation also has an extra symmetry, which we call the "diminished-radix complement"; this symmetry leads to some new pairings of CA rules. We have also discussed the dynamical properties of ECA and 5TCA rules using some structural parameters of the network theory. The results of efficiency [15, 16] and cluster coefficients (CCs) [17, 18] showed that the topological nature of networks could be related to the dynamical behavior of CA rules: the network connectivity between cells can represent the existing rate of class III-like chaotic patterns and class II-like fixed or periodic patterns. Class IV rules have intermediate and complex activities with long transient times, called the "edge of chaos" [19]. We

have also observed the scale-free nature of rule $T20$ network. Sample graphs of all non-trivial networks of ECA and 5TCA are provided in [14].

In this article, we propose a network representation of Life as an application of our approach, which is enhanced for its application to two-dimensional (2D) CA and for the visualization of the networks of Life patterns. A pattern's oscillation and motion can be represented by the sequential changes in a corresponding clustered network. The visualization of Life's *rest* state reveals the long range tension between cells as a complex network. We also discuss some structural parameters of the Life network. The efficiency/CC-all-component (C^{all}) chart shows that the behavior of Life is similar to that of the other class IV rules of ECA and 5TCA. As the most important result, we have found a scale-free degree distribution of the derived network from a Life's rest state, which indicates that the scale-free nature of the network representation is an evidence of a fractal structure and SOC.

Section 2 is devoted to extending our network representation to binary 2D CA. Network links are obtained as a visualization of one-cell perturbation effects through a fixed time interval. The directed links imply the directions of the spreading effects of a pattern change. In Section 3, we illustrate some well-known patterns by the corresponding clustered networks. This visualization shows not only the current state of a pattern but also the pattern's potential variability. A Life's rest state is also visualized. The networks of the well-known patterns are mutually connected and configure a complex network. In Section 4, we discuss the results of the network parameters of Life and 1D CA rules. An efficiency/C^{all} chart illustrates the characteristic figures reflecting the global and local connection properties of the derived networks. The network of a Life's rest state has a scale-free degree distribution. A fractal structure of the network is also discussed.

2   Notation and Definitions

2.1   2D Cellular Automata

Here we consider 2D CA to be dynamical systems that consist of a 2D regular grid of cells, each characterized by a finite number of states. Cells are updated synchronously in discrete time steps ac-

cording to a local rule (CA rule). Each cell is connected to its r local neighbors on four-sides, where r is referred to as the radius. Thus, each cell has $(2r+1)^2$ neighbors, including itself. The state of a cell at the next time step is determined from the current states of the neighboring cells:

$$
\begin{aligned}
x_{i,j}(t+1) \;=\; & f_R(x_{i-r,j-r}(t),...,x_{i-r,j+r}(t),\cdots, \\
& x_{i,j-r}(t),...,x_{i,j}(t),...,x_{i,j+r}(t),\cdots, \\
& x_{i+r,j-r}(t),...,x_{i+r,j+r}(t)), \qquad (1)
\end{aligned}
$$

where $x_{i,j}(t)$ denotes the state of cell (i,j) at time t, and f_R denotes the transition function of a rule. The term *configuration* refers to an assignment of states to all cells for a given time; a configuration is denoted by $x(t) = \sum_{(i,j)=(0,0)}^{(N-1,N-1)} x_{i,j}(t)e_{i,j}$, where $e_{i,j}$ represents the (i,j)-th unit vector that satisfies $e_{i,j} \bullet e_{k,l} = \delta_{(i,j),(k,l)}$ (inner product), and N indicates the size of a square grid. Thus, the time transition of configuration $x(t)$ can be denoted by $x(t+1) = f_R(x(t))$, where f_R represents a mapping on the configuration space $\{x\}_N$ with periodic boundary conditions (torus grid). After t time steps, the configuration of cells obtained from an initial configuration $\varphi \equiv x(0)$ is given by

$$
x(t,\varphi) = f_R^t(\varphi). \qquad (2)
$$

In this article, our discussions are focused on Life, which is the most famous *binary* and *outer-totalistic* CA rule with $r = 1$, where outer-totalistic implies that the rule function depends on the sum of the states of the outer neighbors (i.e., all cells except the center cell). If we denote the sum of the eight cell states neighboring a cell (i,j) as $\sigma_8(i,j)$, the Life rule function f_L can be described as follows:

$$
f_L(x_{i,j}(t),\sigma_8(i,j)) = \begin{cases} 0 & \text{for } \sigma_8 = 1 \text{ or } 4 \sim 8 \\ x_{i,j}(t) & \text{for } \sigma_8 = 2 \\ 1 & \text{for } \sigma_8 = 3. \end{cases}
$$
$$
(3)
$$

2.2   Network Representation

Our network representation is derived from the one-cell perturbation of all cells. The time evolution of each perturbation defines the directed links between the cells. Although the moment of adding perturbations is fixed at the initial time $t = 0$ in our

previous papers, we introduce a parameter t_0 as a moment when all cells are perturbed in order to describe the changing patterns on the basis of the time dependence of the derived networks. If the configuration at t_0 is denoted by $\varphi_0 \equiv x(t_0)$, a one-cell perturbation of cell (i,j), denoted by $\Delta_{i,j}\varphi_0$, coincides with $e_{i,j}$ in *binary* CA. After an interval of time steps t_I, we have

$$
\begin{aligned}
\Delta_{i,j}x(t,\varphi) &\equiv f_R^{t_I}(\varphi_0 + \Delta_{i,j}\varphi_0) + f_R^{t_I}(\varphi_0)\,(\text{mod } 2) \\
&= \Delta_{i,j}f_R^{t_I}(\varphi_0) \qquad\qquad\qquad (4) \\
&= A_R(t_I,\varphi_0) \bullet e_{i,j}, \qquad\qquad (5)
\end{aligned}
$$

where $t = t_0 + t_I$ is the total time steps, and

$$
A_R(t_I,\varphi_0) \equiv \sum_{(k,l)=(0,0)}^{(N-1,N-1)} \Delta_{k,l}f_R^{t_I}(\varphi_0)e_{k,l} \qquad (6)
$$

is the result of gathering all perturbation effects after the interval t_I. $A_R(t_I,\varphi_0)$ has an $N^2 \times N^2$ matrix representation,

$$
[A_R]_{i,j}^{k,l} = (\Delta_{k,l}f_R^{t_I}(\varphi_0))_{i,j}. \qquad (7)
$$

If $\mathcal{N} \equiv \{e_{i,j}\}$ denotes a set of nodes, then each component $(\Delta_{k,l}f_R^{t_I}(\varphi_0))_{i,j}$ defines a one-to-one mapping, i.e., $\mathcal{N} \to \mathcal{N}$. Therefore, we can call $(\Delta_{k,l}f_R^{t_I}(\varphi_0))_{i,j}$ a directed link from node (k,l) to node (i,j). Then, $(\mathcal{N},\mathcal{N},\Delta_{k,l}f_R^{t_I}(\varphi_0))$ defines a directed graph that connects node (k,l) to the other nodes. Taking into consideration all the graphs, we define a network representation of CA as $(\mathcal{N},\mathcal{N},A_R(t_I,\varphi_0))$; the matrix representation of $A_R(t_I,\varphi_0)$ is an *adjacency matrix*.

It is important to determine the appropriate length of the interval t_I. In the previous papers, t_I was set to $[N/2r]$, where $[n]$ represents the maximum integer not exceeding n, in order to ensure that each cell has causal relationships with all the other cells and to avoid repetitions. If a relatively small value were set, such links could not have existed with their lengths longer than $t_I r$ and if a relatively large value were considered, the results would be affected by the lattice size N. Therefore, $[N/2r]$ is a reasonable choice when we consider the time evolution of all the cells from the random initial configurations. A choice of small t_I, however, is appropriate for targeting localized patterns or an intermediate growth of networks, as shown in the following section.

3   Visualization of Life

3.1   Network of Life Patterns

We present some network examples of well-known patterns in Life, including the simplest static patterns, "still lifes" (Figures 1 and 2); repeating patterns, "oscillators" (Figures 3-5); and patterns that moving across the grid, "spaceships" (Figure 6). In these figures, the blue and the white squares represent the active and the inactive cells, respectively. Directed links are drawn with a gradient color from red to blue. Red denotes that the link is exiting the node (*out*-edge), and blue denotes that the link is entering the node (*in*-edge).
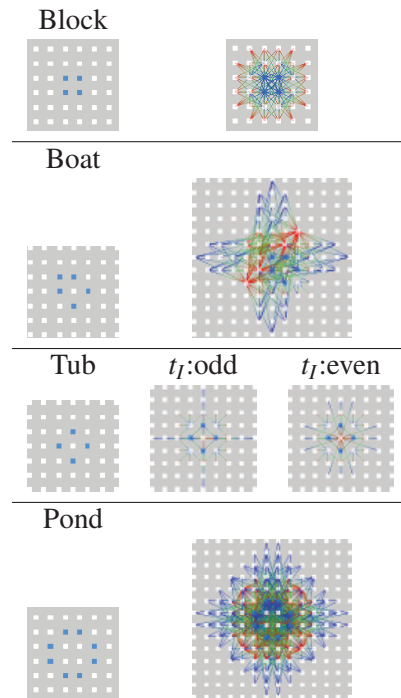

Figure 1. Still lifes, whose networks stop growing at some t_I value. Tub depends on t_I parity.
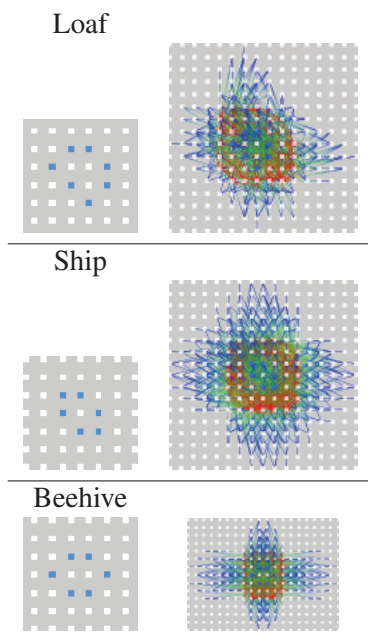
Loaf

Ship

Beehive

Figure 2. Still lifes, whose networks grow with t_I. Networks were obtained at $t_I = 20$.

Among still lifes, the networks of Figure 1 do not grow further if the interval t_I is sufficiently large to construct their networks. Tub depends only on the parity of t_I. On the other hand, the links in the networks of Figure 2 still grow with t_I. We observe that the networks of Figure 2 are surrounded by blue edges (*in*-edges). Because the outer *in*-edges indicate the spreading of the perturbations of the inner cells to the outer area, if a large value of t_I is taken, the blue edges may spread to wide outer areas. These blue edges imply creation of some spaceships and can connect still lifes existing in a *rest* state as discussed in the next subsection.

Blinker t_I:odd t_I:even
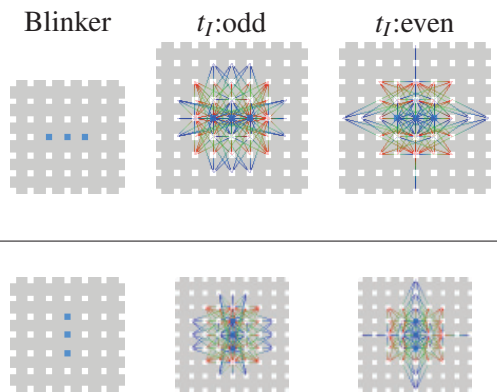
Figure 3. Blinker and oscillating networks (period 2), which are independent of t_0 and depend only on t_I parity.
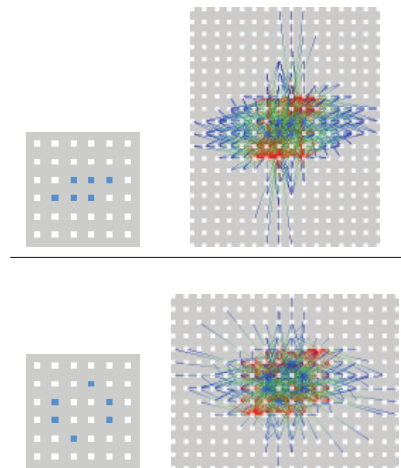

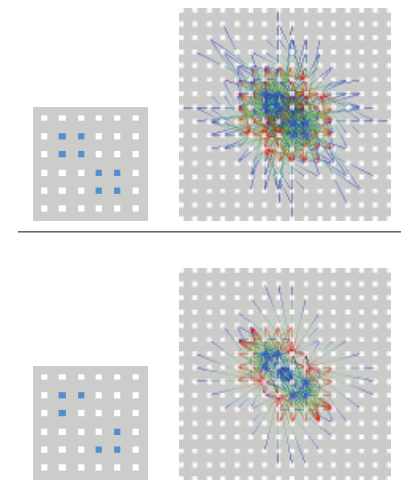**Figure 4**. Toad and oscillating networks (period 2) at $t_I = 20$.

Figure 5. Beacon and oscillating networks (period 2) at $t_I = 20$.

Figures 3-5 show the networks of the famous two-period oscillators. Blinker (Figure 3) has two series of networks depending only on the parity of t_I. The most famous spaceship is Glider (Figure 6) with a period of four. Its networks show the direction of movement because the area where blue links converge indicates the current position of the pattern and the area where the red links converge indicates the t_I past position of the pattern.
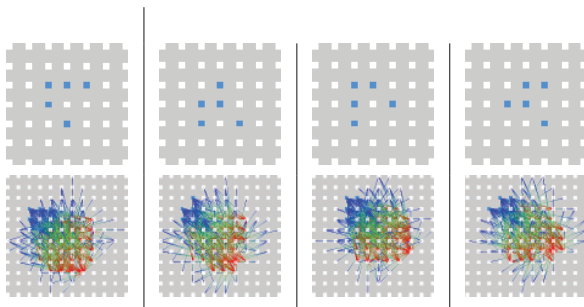
Figure 6. Glider and moving networks (period 4)
at $t_I = 12$.

3.2 Network of Rest State

The initial time t_0 introduced in Section 2 leads us to visualizing the network of the *rest* state of Life. If t_0 is set to a sufficiently large value, the configuration state derived from a randomly generated original state will become a rest state, in which there exist only still lifes and oscillators. When the rest state is visualized by the network representation, we notice a large difference between the rest state and the null state. As mentioned in the previous subsection, Life patterns generally have extending networks with the interval t_I. This implies that the isolated patterns are *not* isolated but are underlying networks that potentially connect many patterns together. Figure 7 shows a sample Life network in a rest state.
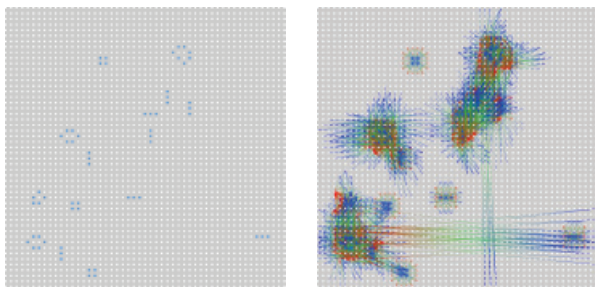

Figure 7. Life's rest state and its network with
$N = 51$ and $t_I = 25$.

The network is almost connected and complex. It describes the long range tension of the rest state as the "sand-pile model" discussed in Bak et al. [12].

4 Network Parameters

We now focus on some structural parameters of the Life network. Figure 8 shows the t_0-dependence

of efficiency and C^{all} of networks derived from Life as well as typical ECA and 5TCA rules, where t_0 is the moment when all cells are perturbed.
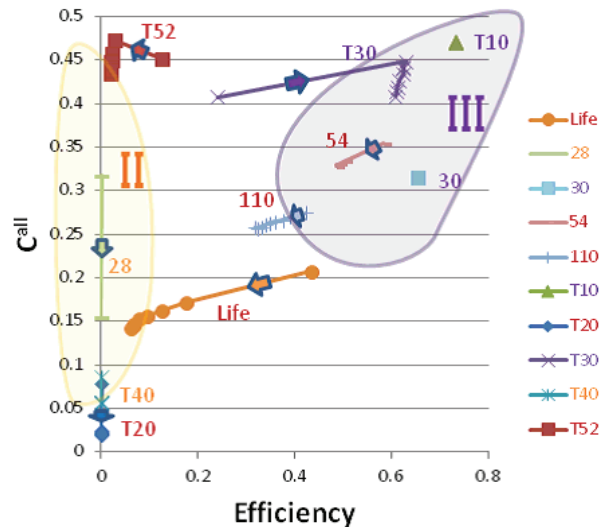

Figure 8. Efficiency/C^{all} graph of Life and some ECA and 5TCA networks. The points of each trajectory correspond to the values at $t_0 = 0 - 400$ at 50 intervals and each point is averaged over ten networks obtained from pseudo-randomly generated initial configurations with $N = 101$ (101×101 total cells), $t_I = 50$ for Life and $N = 3201$, $t_I = 1600$ for ECA and 5TCA. The arrows on the trajectories indicate the direction of the t_0 increase.
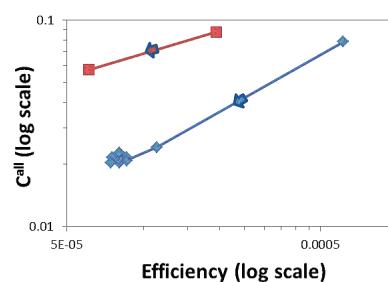

Figure 9. Enlarged efficiency/C^{all} graph of $T20$ and $T40$ networks with a log-log scale.

There is an obvious difference between the trajectories of class II rules (28 and $T40$) and those of class III rules (30, $T10$, and $T30$). The former rapidly fall into fixed points located in the area where both efficiency and C^{all} are small, whereas the latter randomly fluctuate in the area where both the parameters have large values. These activi-

ties correspond to periodic or fixed attractors and chaotic attractors, respectively. Life and the remaining trajectories have similar complex figures with a gradual decrease in efficiency. The rule $T20$ trajectory is also similar, as illustrated in Figure 9.

Because Life and the remaining rules are known as candidates for class IV rules, this chart serves as evidence to prove the validity of our approach. When we focus on Life's trajectory, the fluctuating states have a certain amount of efficiency and C^{all} values. These results indicate that the rest state of Life has somewhat long distance connections and local clusters, which correspond to the results of the visualization of a rest state discussed in Section 3.2.

Figure 10 shows the *in*- and *out*-degree distributions of Life networks.
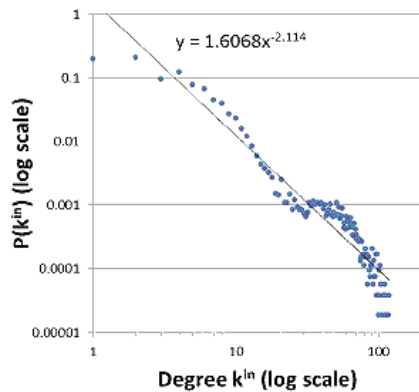
(a) *In*-degree distribution.
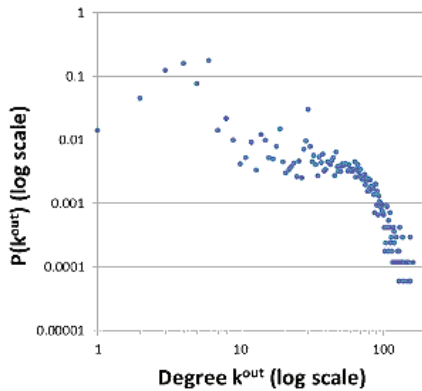
(b) *Out*-degree distribution.

Figure 10. Non-averaged (a) *in*-degree and (b) *out*-degree distributions of Life networks obtained from ten pseudo-randomly generated initial configurations with $N = 101$. t_0 and t_I are set to 10000 and 50, respectively.

In particular, the *in*-degree distribution shows a *scale-free nature*. Here we set t_0 to a sufficiently

large value in order to set the configuration that will be perturbed to an almost rest state. The difference between *in*- and *out*-degree can be interpreted as follows: The *in*-degree of a cell is the number of cells whose perturbations affect the cell after an interval t_I. On the other hand, the *out*-degree of a cell is the number of cells whose states are changed by the effect of the cell's perturbation. For example, Beehive has a characteristic *out*-degree distribution (Figure 11). That is, the *out*-degree of the perturbed cell strongly depends on the local patterns. On the other hand, the *in*-degree is a result of gathering the effects around the cell. The larger the value of the interval t_I, the higher is the randomness of the locations of linked cells; hence, the *in*-degree distribution is more statistical than the *out*-degree distribution.
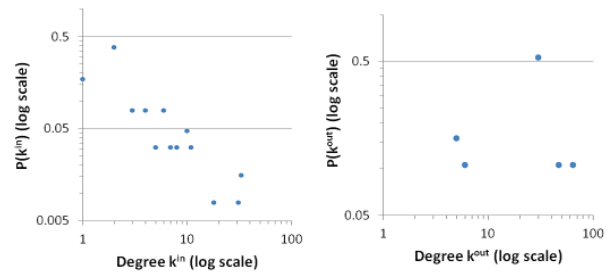

Figure 11. *In*- and *out*-degree distributions of Beehive at $t_I = 50$.

Moreover, if the scale-free nature exists, we expect to observe a fractal structure of the Life network. As noted at the end of Section 2, intermediate networks can be obtained by setting t_I to values smaller than $[N/2]$. In fact, Figure 12 shows a similar power-law behavior even at the smaller t_I values.

The scale-free nature of Life has already been reported by Bak, Chen and Creutz [11], and supported by Alstrn et al. [20]. They have estimated the size and lifetime of an "avalanche", which is defined as an evolutionary change caused by a one-cell perturbation in a rest state. Our approach is very close to theirs and the relation between their results and the Life network will be cleared in the future.
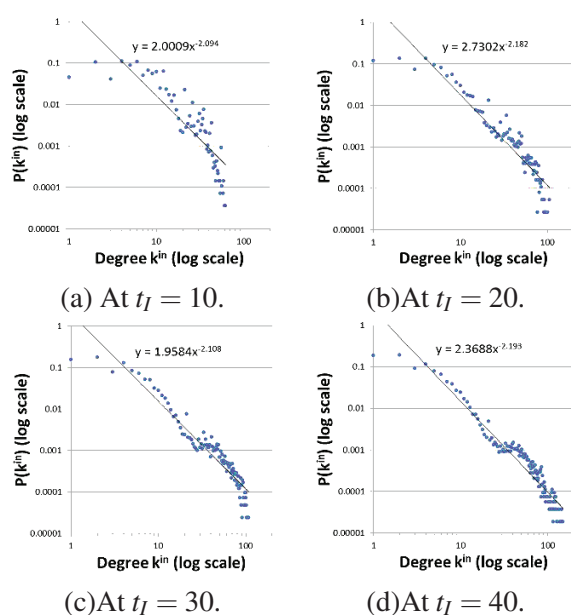
(a) At $t_I = 10$.

(b) At $t_I = 20$.

(c) At $t_I = 30$.

(d) At $t_I = 40$.

Figure 12. *In*-degree distributions of Life networks for different intervals t_I, which are non-averaged data obtained from ten pseudo-randomly generated initial configurations with $N = 101$. t_0 and t_I are set to 10000 and $10 - 40$ at 10 intervals, respectively.

5 Conclusion

Our network representation serves as a novel means of visualizing Life. Well-known Life patterns exhibit characteristic network graphs. There exist two types of networks: ones that grow with time and the others that do not. Block and Blinker are examples of the latter type of networks. Oscillators and spaceships are described by sequential changes in the corresponding clustered networks. Because directed links between cells illustrate potential variability, such as in an infection map or a contour map, the effects of a perturbation will spread along the links. Glider's network implies its direction of movement. Not only individual patterns but also Life's *rest* state made from still lifes and oscillators has been visualized. The network of Life's rest state reveals the existence of underlying high and long-range tension.

The dynamical activities of Life have been studied using structural network parameters. The candidates of Wolfram's class IV rules, including Life, have shown similar trajectories in an efficiency/C^{all} chart. As the most important result, we have found a scale-free degree distribution of the derived network from Life's rest state. As in the case of the

sand-pile model discussed in Bak et al. [12], the underlying tension of Life's rest state has a scale-free nature [11, 20]. The occurrence of an avalanche from a tiny perturbation is the necessary consequence of the power-law structure of a rest state. Now, we conjecture that *the scale-free nature of the network representation is evidence of SOC*. Further investigation into this conjecture will be presented in a future work.

The network representation is a visualization of a connecting structure and its dynamics. The dot patterns of CA rules are illustrated by network graphs which have characteristic connection patterns derived from the dynamical behavior of the corresponding CA rules. As stated in this article, Life is a very good case study for learning how to use the network representation as a tool for understanding complex systems.

Acknowledgment

References

[1] E. R. Berlekmp, J. H. Conway, and R. K. Guy, *Winning Ways for Your Mathematical Plays*. Academic, New York, 1982.

[2] P. Callahan, "What is the game of life?." in Wonders of Math on math.com, http://www.math.com/students/wonders/life/life.html.

[3] A. Flammenkamp, "Most seen natural occurring ash objects in game of life." *http://wwwhomes.uni-bielefeld.de/achim/freq_top_life.html*, 2004. Retrieved at November 1, 2009.

[4] Wikimedia The Free Encyclopedia, "Conway's game of life." http://en.wikipedia.org/wiki/Conway's_Game_of_Life, 2000. Retrieved at August 29, 2011.

[5] J. von Neumann, "The theory of self-reproducing automata," in *Essays on Cellular Automata* (A. W. Burks, ed.), University of Illinois Press, 1966.

[6] P. B. Hansen, "Parallel cellular automata: A model program for computational science," *Concurrency: Practice and Experience*, vol. 5, pages 425–448, 1993.

[7] G. B. Ermentrout and L. Edelstein-Keshet, "Cellular automata approaches to biological modelling," *J. Theor. Biol.*, vol. 160, pages 97–133, 1993.

[8] N. Ganguly, B. K. Sikdar, A. Deutsch, G. Canright, and P. P. Chaudhuri, "A survey on cellular automata," tech. rep., Centre for high performance computing, Dresden University of Technology, 2003.

[9] B. Chopard and M. Droz, *Cellular Automata Modeling Of Physical Systems*. Cambridge University Press, 2005.

[10] S. Wolfram, "Statistical mechanics of cellular automata.," *Rev. Mod. Phys.*, vol. 55, pages 601–644, 1983.

[11] P. Bak, K. Chen, and M. Creutz, "Self-organized criticality in the 'game of life'," *Nature (London)*, vol. 342, p. 780, 1989.

[12] P. Bak, C. Tang, and K. Wiesenfeld, "Self-organized criticality: an explanation of 1/f noise," *Physical Review Letters*, vol. 59 (4), pages 381–384, 1987.

[13] Y. Kayama, "Complex networks derived from cellular automata." arXiv:1009.4509, 2010.

[14] Y. Kayama, "Network representation of cellular automata," in *2011 IEEE Symposium on Artificial Life (IEEE ALIFE 2011) at SSCI 2011*, pages 194–202, 2011.

[15] V. Latora and M. Marchiori, "Efficient behavior of small-world networks," *Phys. Rev. Lett.*, vol. 87-90, pages 198701–198704, 2001.

[16] S. Boccaletti, V. Latora, Y. Moreno, M.Chavez, and D.-U. Hwang, "Complex networks: Structure and dynamics," *Physics Reports*, vol. 424, pages 175–308, 2006.

[17] S. Wasserman and K. Faust, *Social Network Analysis*. Cambridge University Press, 1994.

[18] G. Fagiolo, "Clustering in complex directed networks," *Phys. Rev. E*, vol. 76, pages 026107–026114, 2007.

[19] C. G. Langton, "Computation at the edge of chaos," *Physica D*, vol. 42, pages 12–37, 1990.

[20] P. Alstrøn and J. Leãon, "Self-organized criticality in the "game of life"," *Phys. Rev. E*, vol. 49, pages R2507–R2508, 1994.